Cell Transplantation, Vol. 21, pp. 1651–1665, 2012

0963-6897/12 $90.00 + .00
DOI: http://dx.doi.org/10.3727/096368912X647234
E-ISSN 1555-3892
www.cognizantcommunication.com

Therapeutic Potential of Anterior Cruciate Ligament-Derived Stem Cells for Anterior Cruciate Ligament Reconstruction

Yutaka Mifune,*†‡ Tomoyuki Matsumoto,*†‡ Shusuke Ota,*† Makoto Nishimori,*† Arvydas Usas,*† Sebastian Kopf,*† Ryosuke Kuroda,‡ Masahiro Kurosaka,‡ Freddie H. Fu,† and Johnny Huard*†§

*Stem Cell Research Center, Children's Hospital of Pittsburgh, Pittsburgh, PA, USA
†Department of Orthopedic Surgery, University of Pittsburgh, Pittsburgh, PA, USA
‡Department of Orthopedic Surgery, Kobe University Graduate School of Medicine, Kobe, Japan
§Departments of Molecular Genetics and Biochemistry, and Bioengineering, University of Pittsburgh, Pittsburgh, PA, USA

We recently reported that the ruptured regions of the human anterior cruciate ligament (ACL) contained vascular-derived stem cells, which showed the potential for high expansion and multilineage differentiation. In this study, we performed experiments to test the hypothesis that ACL-derived $CD34^+$ cells could contribute to tendon–bone healing. ACL-derived cells were isolated from the rupture site of human ACL by fluorescence-activated cell sorting. Following ACL reconstruction, immunodeficient rats received intracapsular administration of either ACL-derived $CD34^+$ cells, nonsorted (NS) cells, $CD34^-$ cells, or phosphate-buffered saline (PBS). We also performed in vitro cell proliferation assays and enzyme-linked immunosorbent assays for vascular endothelial growth factor (VEGF) secretion. We confirmed the recruitment of the transplanted cells into the perigraft site after intracapuslar injection by immunohistochemical staining at week 1. Histological evaluation showed a greater area of collagen fiber formation and more collagen type II expression in the $CD34^+$ group than the other groups at the week 2 time point. Immunostaining with isolectin B4 and rat osteocalcin demonstrated enhanced angiogenesis and osteogenesis in the $CD34^+$ group at week 2. Moreover, double immunohistochemical staining for human-specific endothelial cell (EC) and osteoblast (OB) markers at week 2 demonstrated a greater ability of differentiation into ECs and OBs in the $CD34^+$ group. Microcomputerized tomography showed the greatest healing of perigraft bone at week 4 in the $CD34^+$ cell group, and the failure load of tensile test at week 8 demonstrated the greatest biomechanical strength in the $CD34^+$ group. Furthermore, the in vitro studies indicated that the $CD34^+$ group was superior to the other groups in their cell proliferation and VEGF secretion capacities. We demonstrated that ACL-derived $CD34^+$ cells contributed to the tendon–bone healing after ACL reconstruction via the enhancement of angiogenesis and osteogenesis, which also contributed to an increase in biomechanical strength.

Key words: Anterior cruciate ligament; Stem cells; Reconstruction; Tendon–bone healing; Angiogenesis; Osteogenesis

INTRODUCTION

Anterior cruciate ligament (ACL) rupture is one of the most common knee injuries in sports medicine. Approximately 100,000 ACL reconstructions are performed annually in the United States alone (12). In most cases, spontaneous ACL healing fails to take place and reconstruction of the ACL is required, which has become a routine surgical procedure under arthroscopic observation. Whereas most surgical procedures for ACL reconstruction require the tendon grafts to heal in a surgically created bone tunnel, the attachment between the tendon and the bone is the weakest region in the early posttransplantation period (3–5,10). Indeed, it has been reported that the mechanical properties of the healing ligament do not return to normal 1 year after ACL reconstruction surgery in both rabbit and canine models (37,39). Furthermore, Delay et al. reported a human case of ACL reconstruction in which the core portion of the patellar tendon graft remained necrotic 18 months after surgery (9). The lack of vascularity within the ACL graft may induce degeneration or microruptures of the grafted tendon during the postoperative period (36). Therefore, in this surgery using tendon grafts, the tendon graft's ability to heal to the bone is one of the important key factors for successful reconstruction and an early return to normal activity. Some recent articles have shown that the enhancement of angiogenesis, using cytokines or growth factors, led to prompt tendon–bone healing

Received December 17, 2010; final acceptance September 30, 2011. Online prepub date: June 20, 2012.
Address correspondence to Johnny Huard, Ph.D., Stem Cell Research Center, Children's Hospital of Pittsburgh, Department of Orthopedic Surgery, University of Pittsburgh, 450 Technology Drive, 2 Bridgeside Point, Suite 206, Pittsburgh, PA 15219, USA. Tel: +1 412-648-2641; E-mail: jhuard@pitt.edu

(15,31,41). On the other hand, stem/progenitor cells, such as endothelial progenitor/CD34$^+$ cells, have also been used and shown to promote neovascularization in the ischemic area (6,16,18,19), and these stem cells have been generally considered to be a promising cell source for tissue regeneration treatments because of their potential for high levels of expansion, self-renewal, and multipotent differentiation capacities. Recently, blood vessels have been reported to possess a rich supply of stem/progenitor that express the cell surface markers CD34 (8,14,35,42). Our laboratory has also identified and purified, via flow cytometry, the cell population that are developmentally and anatomically related to the blood vessel walls in human tissues. This population of cells can be found in the skeletal muscle, including myoendothelial cells that coexpress markers of endothelial and myogenic cells (CD34 and CD56). Also, this population exhibits multilineage developmental potentials, in culture and in vivo, and has been shown to differentiate into skeletal myofibers, bone, cartilage, and adipocytes (7,8,42). Moreover, we recently reported that the ruptured and septum regions of the human ACL contained numerous vascular-derived stem cells and that ACL-derived CD34$^+$ cells showed potentials for high expansion and multilineage differentiation capacities (26). Based on these latter findings, we performed experiments to test the hypothesis that the transplantation of human ACL-derived CD34$^+$ cells derived from the site of ACL rupture could contribute to tendon–bone healing and regeneration.

MATERIALS AND METHODS

Samples

Human adult ACL-ruptured tissues were harvested from subjects undergoing arthroscopic primary ACL reconstruction after informed consents by all patients (22.5 ± 3.8 years old, 5.1 ± 1.9 months postinjury, $n = 8$). The rupture sites of all samples were at the femoral attachment sites. The IRB protocols were approved by the institutional review board at the University of Pittsburgh.

Cell Isolation

The human adult ACL tissues were transported in sterile saline solution on ice. The excised ACL tissues were dissected into two regions, the rupture site and the midsubstance site. The tissues were minced into small pieces approximately 1–2 mm^3, washed three times in phosphate-buffered saline (PBS) (Sigma Aldrich, St. Louis, MO), and were then digested with 0.4% collagenase type I (0.4% w/v) (Invitrogen, Carlsbad, CA) in Dulbecco's modified Eagle's medium (DMEM) (Sigma) supplemented with 10% fetal bovine serum (FBS) (Invitrogen) and 1% penicillin/streptomycin (standard medium) (Invitrogen) for 4–6 h. Cells were spun down, resuspended in medium, passed through a 70-μm pore size nylon filter (BD, Bedford, MA), and washed twice with the same type of medium. Isolated cells from each region were cultured for 2–3 days in the standard DMEM medium.

These cells were first incubated with mouse serum (Sigma; 1:10) in fluorescence-activated cell sorter (FACS) buffer (BD Pharmingen, Bedford, MA) for 10 min on ice and were then incubated with CD34-allophycocyanin (APC; BD Pharmingen) for 30 min. To exclude dead cells, 7-aminoactinomycin D (Via-probes, BD Pharmingen) was added to each tube. Live cells were analyzed using a FACS Aria Cell-Sorting System (BD) and Cell Quest software (BD). After examining the cell marker profiles, the cells were gated out and CD34$^+$ and CD34$^-$ cells were sorted following a protocol described by Zheng et al. (42) and Crisan et al. (8), as shown in our previous study (26).

Animal Model of ACL Reconstruction

A reproducible model of ACL reconstruction was created in immunodeficient rats with autologous flexor digitorum longus tendon as a graft according to a previous report (20). The animal experiments conducted as a part of this study were approved by the Institutional Animal Care and Use Committee in University of Pittsburgh. Forty 10-week-old female nude rats (NIH-Whn NIHRNU-M; Taconic, Germantown, NY) were used for these experiments. The animals were anesthetized with 3% isoflurane and O_2 gas (1.5 L/min) delivered through an inhalation mask. A longitudinal incision was made on the medial aspect of the distal leg and ankle, and the flexor digitorum longus tendon was identified and then cut just distal to the ankle. The full length of the flexor digitorum longus tendon (average length, 20 mm) was harvested. A second incision was made over the knee, a lateral parapatellar arthrotomy was performed, and the native ACL was excised. Using an 18-gauge needle, a bone tunnel was made in the proximal tibia and the distal femur, entering the joint at the attachment sites of the ACL. A 4-0 Ethibond suture (Ethicon, Somerville, NJ) was passed through each end of the previously harvested tendon graft, and then the graft was passed through the bone tunnels to replace the ACL. Both ends of the grafted tendon were secured to the surrounding periosteum at the extra-articular tunnel exit site at the distal femur and proximal tibia using 4-0 Ethibond suture. The wounds were closed in routine fashion. It took approximately 10 min to perform the ACL reconstruction surgical procedure, and then the animals were allowed ad lib activity postoperatively.

Cell Transplantation

Three days after ACL reconstruction, the rats received a 50-μl intracapsular injection of one to the following: (1) ACL-derived CD34$^+$ cell: 5×10^5 cells (CD34$^+$ group) in PBS, (2) ACL-derived nonsorted (NS) cell: 5×10^5 cells (NS group) in PBS, (3) ACL-derived CD34$^-$ cell: 5×10^5 cells (CD34$^-$ group) in PBS, or (4) no cells (PBS only) (PBS group).

Tissue Harvest

Rats were euthanized by CO_2 overdose. The femur–graft–tibia complexes were harvested and quickly embedded in optimal cutting temperature (OCT) compound (Miles Scientific, Elkhardt, IN), snap frozen in liquid nitrogen, and stored at −80°C for histochemical and immunohistochemical staining as described below.

Histological Examination

The embedded femur–graft–tibia complexes were sectioned at 6 μm, and the serial sections were mounted on silane-coated glass slides (Sigma) and air dried for 1 h before being fixed with 4% paraformaldehyde at 4°C for 5 min and then stained immediately. Hematoxylin and eosin (H&E) staining was performed to identify the interface zone between the grafted tendons and bone following standard protocols. Also, tissue sections were stained with Masson's trichrome elastin to identify collagen fibers at week 2 ($n=6$ in each group) according to standard operating procedures.

Quantification of Collagen Fibers

The areas of the entire visible tendon–bone interface and collagen fibers within the interface were measured, respectively, in histological sections stained with Masson trichrome by Scion Image analysis software (Scion Corporation, Frederick, MD), which is based on the popular NIH image J software originally designed for the Macintosh platform. The collagen fiber area was divided by the tendon–bone interface area to obtain the proportion of the collagen fibers to the entire tendon–bone interface. Three sections were examined per specimen, and the quantification of collagen fibers was analyzed by three blinded examiners who were not informed of the group assignment.

Immunofluorescence Staining to Detect Chondrocytes at the Interface Zone

To detect chondrocytes at the interface zone between the bone-ligament junction, immunofluorescent staining for type II collagen (Col2) was performed at the 2 week time point using rabbit anti-rat Col2 antibody (Sigma) to detect chondrocytes and Alexa Fluor 594-conjugated donkey anti-rabbit IgG (Molecular Probes, Eugene, OR) at a 1:200 dilution as a secondary antibody. The numbers of Col2-positive cells were morphometrically counted in five randomly selected soft tissue fields using Northern Eclipse software (Empix Imaging, Inc., Cheektowaga, NY), and the averages were determined.

Immunofluorescent Staining to Detect Transplanted Cells

To trace transplanted human cells in the rat knee joint, immunohistochemistry ($n=4$, in each group) was performed at week 1 with a mouse anti-human nuclear antigen (HNA) antibody (Millipore Corporate Headquarters, Billerica, MA). This anti-HNA antibody was used at 1:100 dilution and incubated at room temperature for 1 h. The secondary antibody used against HNA was Alexa Fluor 594-conjugated goat anti-mouse IgG (Molecular Probes) used at 1:200 dilution and incubated at room temperature for 2 h. 4,6-Diamidino-2-phenylindole (DAPI) solution was applied for 5 min for nuclear counterstaining. After staining, we evaluated the number of double stained cells in five randomly selected fields (250×250 μm) of the tissue at the interface zone between the bone and tendon using Northern Eclipse software (Empix Imaging, Inc., Cheektowaga, NY).

Human Cell-Derived Vasculogenesis and Osteogenesis

To detect transplanted human cells at the interface zone between bone and tendon in the rats, double immunohistochemistry ($n=6$, in each group) was performed at week 2 using a human-specific CD31 (hCD31) antibody (Santa Cruz Biotechnology, Inc., Santa Cruz, CA), a human-specific osteocalcin (hOC) antibody (Abcam, Cambridge, MA), and the HNA antibody to detect human cells and murine-specific endothelial cell (EC) marker isolectin B4-fluorescein isothiocyanate (FITC)-conjugated antibody (Vector Laboratories, Burlingame, CA) to detect mouse ECs (18). The primary antibodies for immunostaining were: hCD31, hOC antigen, HNA, or isolectin B4-FITC conjugate and used at a 1:100 dilution and incubated at room temperature for 1 h. The following fluorophore conjugated secondary antibodies were used against the primary antibodies: Alexa Fluor 594-conjugated goat anti-mouse IgG (Molecular Probes) was used at 1:200 dilution at room temperature for 2 h to detect hCD31 and HNA; Alexa Fluor 488-conjugated goat anti-mouse IgG (Molecular Probes) was used at 1:200 dilution at room temperature for 2 h to detect hOC. DAPI solution was applied for 5 min for nuclear counterstaining. After staining, we evaluated the number of double-stained cells in five randomly selected fields (250×250 μm) of the tissue at the interface zone between the bone and tendon using Northern Eclipse software (Empix Imaging, Inc.).

Morphometric Evaluation of Capillary Density and Osteoblast Density

Using immunohistochemical staining for murine-specific EC marker isolectin B4-FITC conjugate (Vector), a rat-specific endothelial marker, the regenerated capillaries, and/or neovascularity could be visualized and quantified using fluoromicroscopy at week 2 posttreatment ($n=6$ in each group). Regenerated bone and/or newly formed bone were visualized and recognized using an antibody against the rat OC antigen (Santa Cruz), which identified rat osteoblasts (OB) at week 2 posttreatment ($n=6$ in each group). The murine-specific EC marker isolectin B4-FITC conjugate and rat OC antigen were used as the primary antibodies at 1:100 dilution and incubated at room temperature for 1 h. The secondary antibody against the rat OC antibody was Alexa Fluor

488-conjugated donkey anti-goat IgG (Molecular Probes) used at a 1:200 dilution and incubated at room temperature for 2 h. After staining, we also evaluated the capillary and OB densities by analyzing five randomly selected fields (250×250 μm) of the tissue at the interface zone between bone and tendon using Northern Eclipse software.

RNA Isolation and Reverse Transcriptase Polymerase Chain Reaction Analysis

Total RNA was extracted from cells or pellets using RNeasy plus Mini Kit (Qiagen) in accordance with the manufacturer's instructions. One microgram of total RNA was used for random hexamer-primed cDNA synthesis using reverse transcription of the SuperScript II preamplification system (Invitrogen). Equal amounts of cDNA synthesis were used as templates for RT-PCR amplification per 25 μl reaction volume using Taq DNA polymerase (Invitrogen) and 50 pmol of gene-specific primers. The sequences and product sizes of the primers for VE-cadherin (VE-cad), CD31, type I collagen (COL I), osteocalcin (OC), and β-actin are listed below. RT-PCR amplifications were performed by preheating the mixture at 95°C for 5 min followed by 35 cycles of 1 min at 95°C, 45 s at 58°C, and 1 min at 72°C. A final extension of 10 min was performed at 72°C. The PCR products were resolved by electrophoresis on 1.5% agarose gels and visualized by ethidium bromide staining. The mRNA expression of β-actin was used to normalize gene expression. Total RNA extracted from fetal bone and human umbilical vein endothelial cells (HUVECs) were used as positive controls for osteogenic and endotheliogenic gene expression. Primers used were hVE-cad (461 bp): sense ACGCCTCTGTCATGTACCAAATCCT and antisense GGCCTCGACGATGAAGCTGTATT; hCD31 (469 bp) (28): sense: AAGTCAAGCAGCATCGTGGTCAACAT and antisense TTGTCTTTGAATACCGCAG; hCOL1 (600 bp): sense TGACGAGACCAAGAACTG and antisense CCATCCAAACCACTGAAACC; hOC (300 bp): sense GTGCAGAGTCCAGCAAAGGT and antisense GCAAGGGGAAGAGGAAAGAA; hβ-actin (205 bp): sense CCTCGCCTTTGCCGATCC and antisense GGA ATCCTTCTGACCCATGC.

Micro-CT Evaluation

The perigraft bone volume was evaluated using a high-resolution micro-CT (μCT-40, Scanco Medical, Brüttisellen, Switzerland) ($n=6$ in each group). The rats were anesthetized with 3% isoflurane and O_2 gas (1.5 L/min) delivered through an inhalation mask and placed with their long axes in the vertical position and immobilized with a foam pad in a cylindrical sample holder. The continuous scans were performed perpendicular to the long axis of the limb at an isotropic resolution of 30 μm^3. A region of interest (ROI) of 6 mm in diameter was user-defined to cover the bone tunnel and the 1 mm of the tibial tunnel from the proximal end was analyzed. The same ROI was used on all of the samples acquired postoperatively from weeks 0, 2, and 4. The acquired 3D data set was convoluted with a 3D Gaussian filter with a width and support equal to 1.2 and 2, respectively. Bone was segmented from the marrow and soft tissue for subsequent analyses using a global thresholding procedure. A threshold equal to or above 210 represented bone tissue; a threshold below 210 represented bone marrow and soft tissue. The bone volume/tissue volume (BV/TV) was evaluated using the built-in software of micro-CT.

Biomechanical Assessment

Eight weeks after surgery, four knees from each group were biomechanically tested. As a control group, four uninjured rat knees were also prepared for biomechanical testing. Before the biomechanical tests, the hind limbs were completely freed of all soft tissue except for the ACL graft, which was carefully dissected. The femur and tibia were cut 20 mm from the joint line, and both femur and tibia were fixed in a cylinder hole of the specially designed aluminum plate using super glue. The prepared femur–ACL–tibia complex was mounted in a conventional tensile tester, DS2 (Imada, Inc, Northbrook, IL), and an applied load was directed along the longitudinal axis of the ACL graft. Before testing, we applied 10 cycles of longitudinal loads of 1 N to the knee specimen as a preconditioning. After preconditioning, each femur–ACL–tibia complex was stretched at a crosshead speed of 0.25 mm/s until gross failure of the ACL occurred. In addition to the tensile tests on the operated knees, biomechanical tests were also performed on healthy femur–ACL–tibia complexes to obtain normal control values. The four normal knees with uninjured ACLs were prepared, tested, and measured in the same way as the experimental specimens. The specimens were kept moist throughout the specimen preparation and testing with physiologic saline solution.

Cell Proliferation Assay

To assess the proliferation ability of the cells in each group, cells were plated at a density of 5×10^3 cells per well in 96-well plates and cultured in Dulbecco's modified Eagle's medium (Sigma) supplemented with 10% fetal bovine serum (Sigma). A media blank (no cells) was also run in parallel as a control. The plate was incubated at 37°C in an atmosphere of 5% CO_2 for 4 days. After cultivation, 20 μl of cell titer 96 Aqueous One Solution (Pomega, Madison, WI) was added to each well, and the plates were then incubated at 37°C in an atmosphere of 5% CO_2 for 3 h to allow the development of color to occur. Absorbance was measured at 490 nm with Infinite 200 NanoQuant and i-control microplate reader software (TECAN, Durham, NC).

Enzyme-Linked Immunosorbent Assay (ELISA) to Detect Vascular Endothelial Growth Factor (VEGF) Secretion

We determined the amount of VEGF secreted into the supernatant by the ACL-derived CD34$^+$ cells, nonsorted cells, and CD34$^-$ cells in vitro by first incubating 1×10^5 of each cell type in collagen coated six-well dish for 48 h and then measuring the amount of VEGF that was secreted by ELISA (R&D Systems, Minneapolis, MN), as previously described (30).

Statistical Analysis

All values are expressed as means ± standard errors. The data were compared by ANOVA test followed by the Tukey's test. A probability value $p<0.05$ was considered to denote statistical significance.

RESULTS

Efficient Incorporation of the Transplanted Cells

To track the transplanted cells following intracapsular injection, immunostaining of the ACL complex for HNA was performed 1 week postinjection to quantify the number of transplanted human cells at the interface zone between the grafted tendon and bone, which is shown in Figure 1A stained with H&E. HNA immunostaining demonstrated an abundant recruitment of the transplanted cells to the bone tunnel site, especially in the CD34$^+$ group (Fig. 1B–E). The number of stained human cells at the bone tunnel was significantly higher in the CD34$^+$ group compared with the other groups, as well as in the NS or CD34$^-$ groups compared with the PBS group (CD34$^+$, 247.3 ± 37.1; NS, 119.3 ± 17.2; CD34$^-$, 68.3 ± 15.9; PBS, 0.0 ± 0.0/mm^2, respectively; $p<0.01$ for CD34$^+$ vs. CD34$^-$ or PBS group, for NS vs. PBS group and for CD34$^-$ vs. PBS group, $p<0.05$ for CD34$^+$ vs. NS group) (Fig. 1F). These morphological findings indicate that ACL-derived CD34$^+$ cells are superior to the other cell groups in terms of efficiency of transplanted cell incorporation into the bone tunnel after intracapsular injection. Note that few transplanted cells were found within other parts of the capsule (data not shown).

Histological Evidence of Bone–Tendon Healing

Histological evaluation was performed with Masson's trichrome staining to assess tendon–bone healing at 2 weeks postinjection. The tendon–bone interface tissue around the grafted tendon was observed to be composed of cellular and vascular fibrous tissue (Fig. 2A–D). The entire visible tendon–bone interface areas and collagen fibers in the interface were measured by Scion Image analysis software. Quantification analysis demonstrated the total collagen fiber area was significantly greater in the CD34$^+$ group than the CD34$^-$ or PBS groups (CD34$^+$, 66.3 ± 6.0; NS, 54.8 ± 8.1; CD34$^-$, 43.0 ± 7.7;

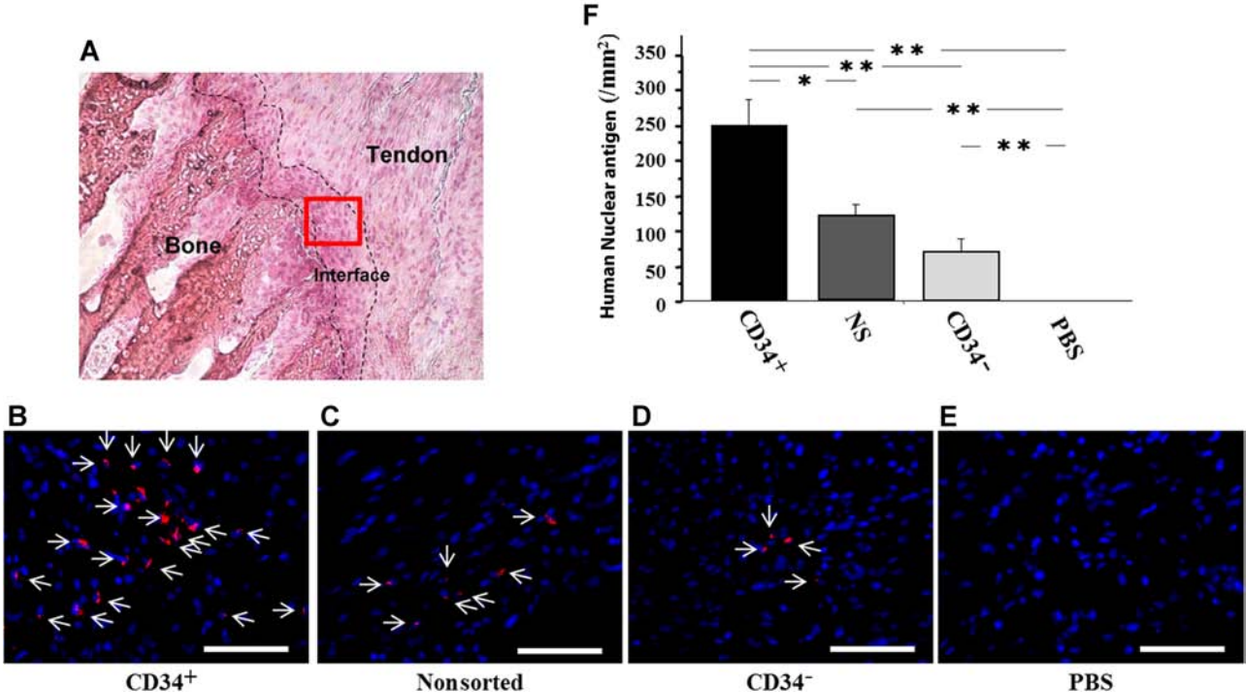

Figure 1. (A) Hematoxylin and eosin (H&E) staining with immunostaining for human nuclear antigen (HNA) (red square) showed the locations of the assessed areas. (B–E) The immunostaining for HNA (red) at week 1 demonstrated abundant recruitment of transplanted cells at the bone tunnel in the CD34$^+$ (B) and nonsorted (NS) group (C), not in the CD34$^-$ (D) or PBS group (E). Arrow, HNA$^+$ cell. Bar: 50 µm. (F) The number of transplanted cells at the bone tunnel was significantly higher in the CD34$^+$ group compared with the other groups, as well as in the NS group better than the CD34$^-$ or PBS group. **$p<0.01$; *$p<0.05$ ($n=4$ in each group).

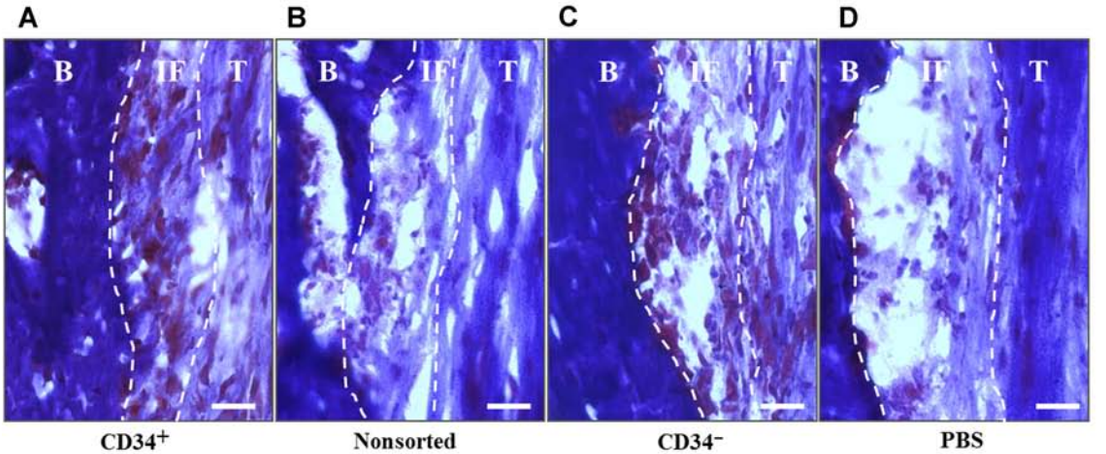
A
B
C
D
B
IF
T
CD34+
Nonsorted
CD34−
PBS

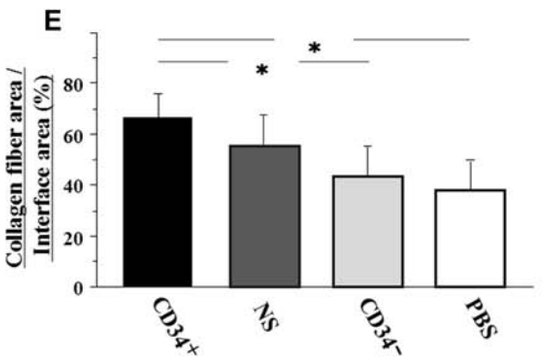
E
Collagen fiber area / Interface area (%)
0
20
40
60
80
*
*
CD34+
NS
CD34−
PBS

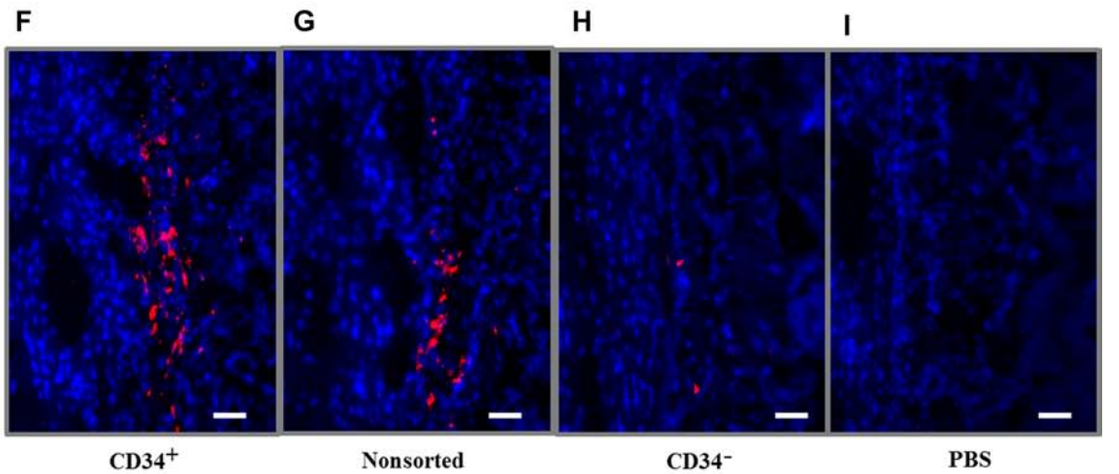
F
G
H
I
CD34+
Nonsorted
CD34−
PBS

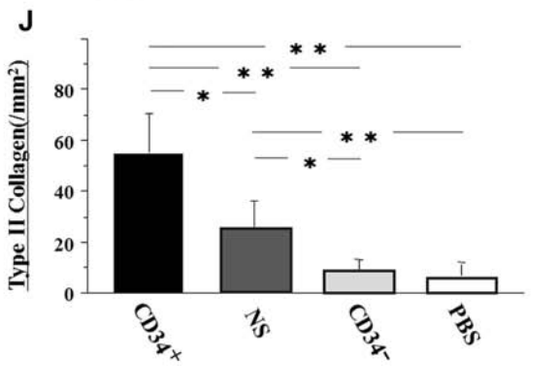
J
Type II Collagen(/mm²)
0
20
40
60
80
* *
* *
* *
CD34+
NS
CD34−
PBS

PBS, 37.3%±7.4%, respectively; $p<0.05$ for $CD34^+$ vs. $CD34^-$ or PBS group). To histologically assess the healing of the bone–ligament junction, immunofluorescent staining for Col2 was performed using tissue samples obtained 2 weeks posttransplantation (Fig. 2F–I). Quantification of the Col2-positive stained cells demonstrated that the number of Col2-positive cells was found to be significantly higher in the $CD34^+$ group when compared to the other groups. Also, the number of Col2-positive cells was significantly higher in the NS group when compared to the $CD34^-$ and PBS groups ($CD34^+$, 56.6±9.0; NS, 27.4±8.1; $CD34^-$, 9.2±1.3; PBS, 6.1±0.9/mm^2, respectively; $p<0.01$ for $CD34^+$ vs. $CD34^-$ and PBS group; $p<0.05$ for $CD34^+$ vs. NS group; $p<0.01$ for NS vs. PBS group; $p<0.05$ for NS vs. $CD34^-$ group) (Fig. 2J).These results indicate that ACL-derived $CD34^+$ cells contribute to rapid tendon osteointegration in the early period after ACL reconstruction.

Enhancement of Intrinsic Vascularization and Osteogenesis

Enhanced angiogenesis and osteogenesis imparted by the transplanted cells on the recipients' cells was confirmed by immunostaining for rat-specific markers. This enhancement is believed to be a paracrine induced effect imparted by the implanted donor cells. Vascular staining with isolectin B4, a rat-specific marker for ECs, using tissue samples collected 2 weeks after ACL reconstruction, demonstrated an enhancement in intrinsic neovascularization around the bone tunnel in animals treated with ACL-derived $CD34^+$ and NS cells (Fig. 3A–D). Capillary density determined by analyzing isolectin B4 was significantly greater in the $CD34^+$ group compared with the other groups, and the NS group was significantly greater compared with the $CD34^-$ and PBS groups ($CD34^+$, 316.5±37.6; NS, 196.5±28.6; $CD34^-$, 113.0±17.9; PBS, 105.8±13.2/mm^2, respectively; $p<0.01$ for $CD34^+$ vs. $CD34^-$ or PBS group, $p<0.05$ for $CD34^+$ vs. NS group and for NS vs. $CD34^-$ or PBS group) (Fig. 3E). OB staining using rat OC antigen demonstrated an enhancement of intrinsic osteogenesis at the perigraft sites in animals treated with ACL-derived $CD34^+$ and NS cells (Fig. 3F–I). OB density, as determined with a rat OC antibody, was significantly greater in the $CD34^+$ group compared with the other groups, and the NS group was significantly greater compared with the $CD34^-$ and PBS groups ($CD34^+$, 147.0±15.2; NS, 71.5±17.5; $CD34^-$, 43.8±15.2; PBS group, 21.8±9.8/mm^2, respectively; $p<0.01$ for $CD34^+$ vs. $CD34^-$ or PBS group, $p<0.05$ for $CD34^+$ vs. NS group and for NS vs. PBS group) (Fig. 3J). These results indicate that ACL-derived $CD34^+$ and NS cells enhance both intrinsic angiogenesis and osteogenesis at the tendon–bone interface zone.

Human Cell-Derived Vasculogenesis and Osteogenesis

Immunohistochemical staining for hEC and hOB markers was performed using the tissue samples harvested at week 2. Differentiated human ECs were identified as hCD31-positive cells at the vascular sites stained with isolection B4 in the $CD34^+$, NS, and $CD34^-$ groups (Fig. 4A–E). The number of human-derived ECs was significantly greater in the $CD34^+$ group compared with the other groups, and the NS group was significantly greater compared with the $CD34^-$ and PBS groups ($CD34^+$, 84.8±10.3; NS, 36.0±11.1; $CD34^-$, 6.8±3.3; PBS, 0.0±0.0/mm^2, respectively; $p<0.01$ for $CD34^+$ vs. the other groups and for NS vs. PBS group, $p<0.05$ for NS vs. $CD34^-$ group) (Fig. 4F). To further verify this phenomenon, RT-PCR analysis of tissue RNA isolated from the peribone tunnel site for human-specific EC markers (hVE-cad and hCD31) was performed. The expressions of hVE-cad and hCD31 were detected in the $CD34^+$ and NS groups (Fig. 4G).

Differentiated hOBs were identified as double positive cells with HNA and hOC in the area of newly formed bone in the $CD34^+$, NS, and $CD34^-$ groups (Fig. 4H–L). The number of human-derived OB cells was significantly greater in the $CD34^+$ group compared with the other groups, and the NS group was significantly greater compared to the $CD34^-$ and PBS groups ($CD34^+$, 43.5±11.0; NS, 21.0±7.5; $CD34^-$, 2.3±1.4; PBS group, 0.0 ± 0.0/mm^2, respectively; $p < 0.01$ for $CD34^+$ vs. $CD34^-$ or PBS group and for NS vs. $CD34^-$ or PBS group, $p<0.05$ for $CD34^+$ vs. NS group) (Fig. 4M). RT-PCR analysis also demonstrated expression of the human-specific bone-related markers (hOC and hCol1) following human $CD34^+$ cell transplantation (Fig. 4N). These results indicate that intracapsslar transplanted ACL-derived $CD34^+$ cells can effectively differentiate into both EC and OB lineages at the tendon–bone interface zone in vivo.

Bone Volume Evaluation by Micro-CT

The perigraft bone volume was evaluated with micro-CT. A transient perigraft bone mass decrease was observed in all groups at week 2. There was no significant difference

FACING PAGE

Figure 2. (A–D) Histological evaluations with Masson's trichrome staining. The tendon–bone interface tissue around the grafted tendon was observed to be composed of cellular and vascular fibrous tissue. The total collagen fiber area was significantly greater in the $CD34^+$ group (A) than the $CD34^-$ (C) or PBS groups. (D) Scale bar: 50 μm. B, bone; IF, interface zone; T, tendon. (E) Quantification analysis demonstrated the total collagen fiber area was significantly greater in the $CD34^+$ group than the $CD34^-$ or PBS group at week 2. $^{**}p<0.01$; $^{*}p<0.05$ ($n=6$ in each group). (F–I) Immunofluorescent staining for type II collagen (Col2) on tissue samples obtained 2 weeks posttransplantation demonstrated better regeneration between the graft and the bones in the $CD34^+$ and NS groups when compared with the other groups. (J) Quantification of the Col2-positive stained cells demonstrated that the number of Col2-positive cells was found to be significantly higher in the $CD34^+$ group when compared to the other groups and that the number of Col2-positive cells was significantly higher in the NS group when compared to the $CD34^-$ and PBS groups. $^{**}p<0.01$; $^{*}p<0.05$ ($n=6$ in each group).

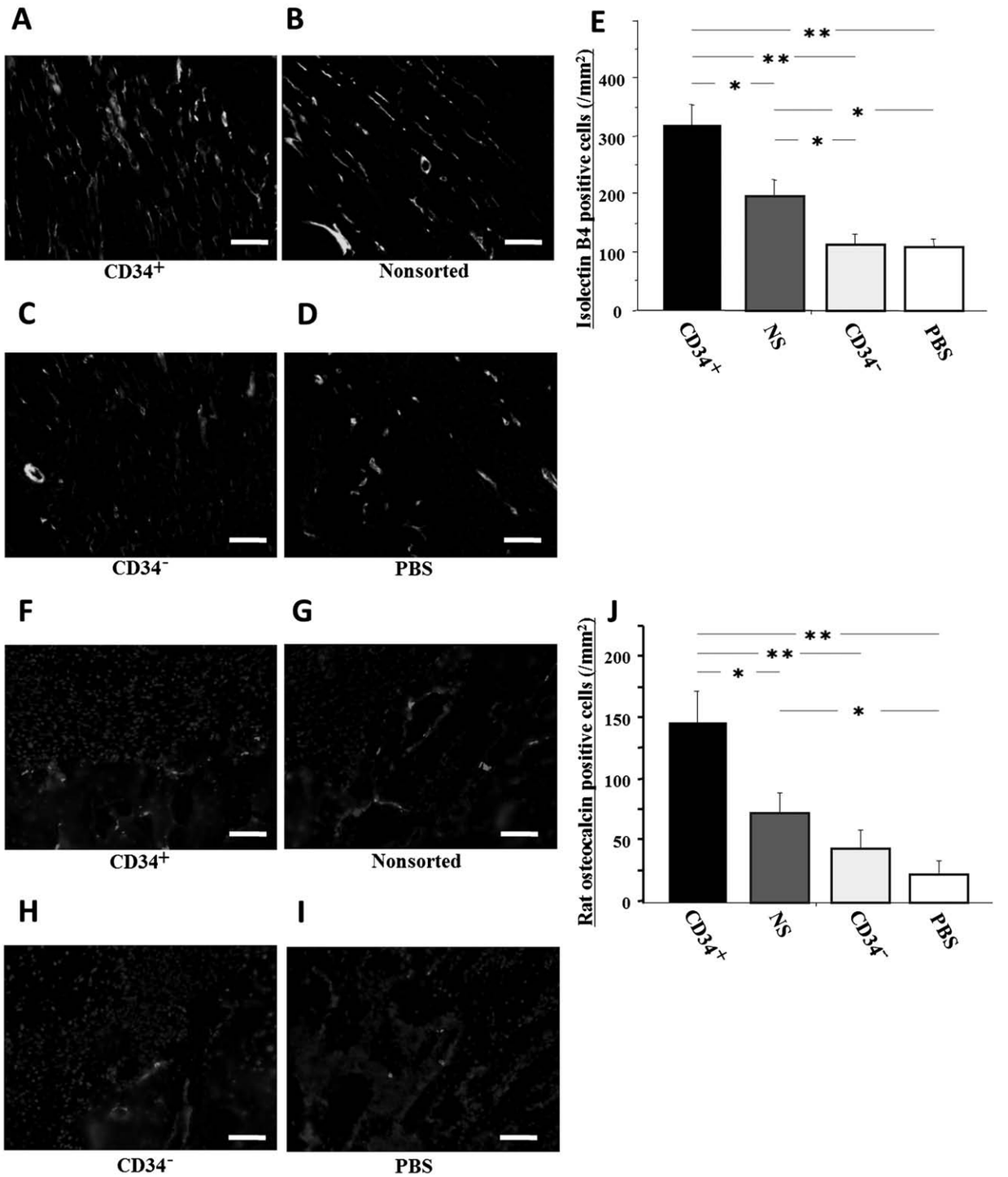

Figure 3. (A–D) Enhancement of neovascularization and osteogenesis by recipient cells following anterior cruciate (ligament) ACL-derived cell transplantation. Representative vascular staining with isolectin B4 using tissue samples collected at week 2. Scale bar: 50 μm. (E) Neovascularization assessed by capillary density at week 2 was significantly greater in the $CD34^+$ group compared with the other groups, as well as in the NS group better than the $CD34^-$ or PBS group $^{**}p<0.01$; $^{*}p<0.05$ ($n=6$ in each group). (F–I) Representative osteoblast (OB) staining with rat osteocalcin (bright spots) at week 2. Scale bar: 50 μm. (J) Osteogenesis assessed by OB density at week 2 was significantly greater in the $CD34^+$ group compared with the other groups, as well as in the NS group compared with the PBS group. $^{**}p<0.01$; $^{*}p<0.05$ ($n=6$ in each group).

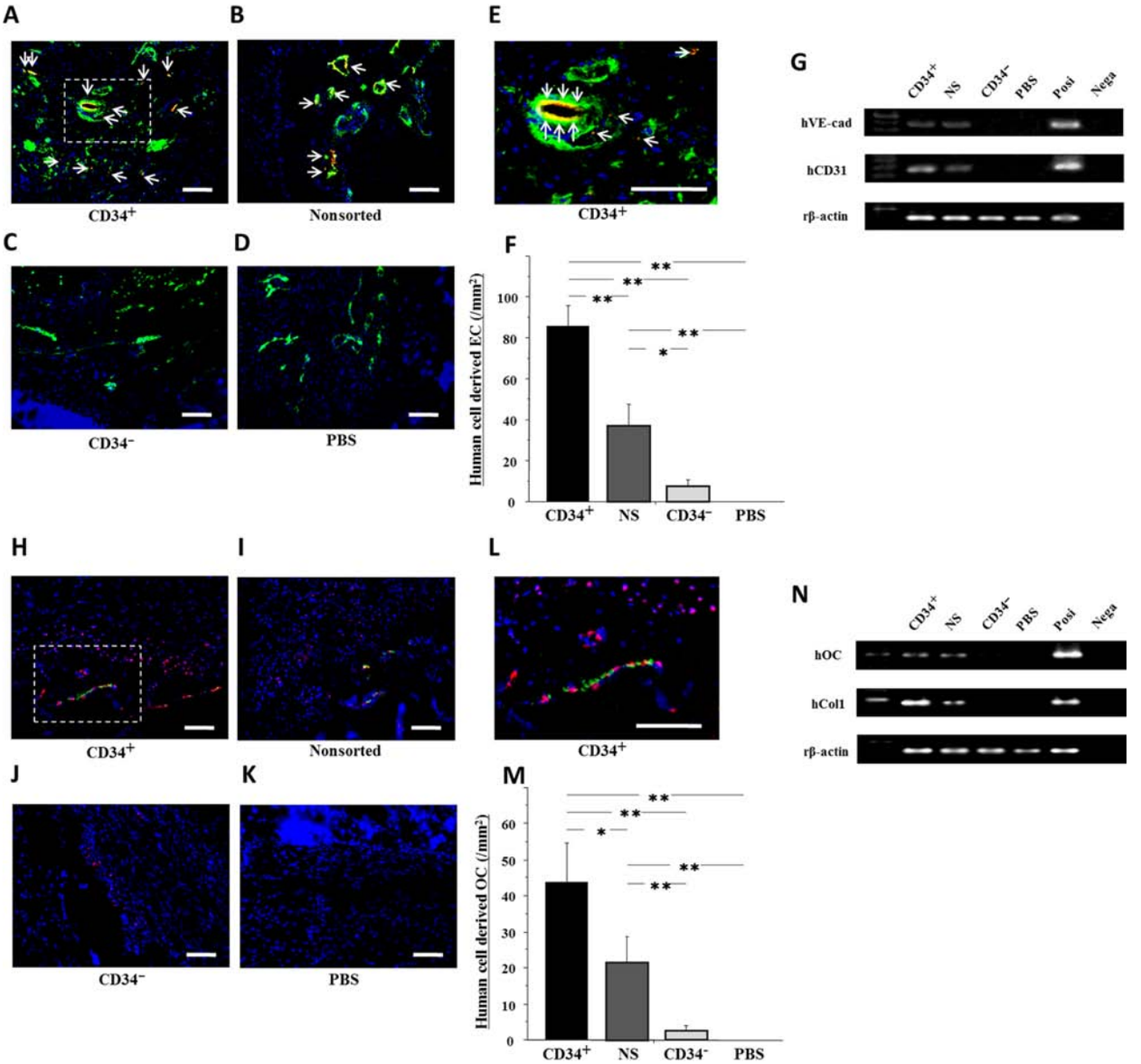

Figure 4. (A–E) Perigraft site vasculogenesis derived from ACL-derived cells. Representative double immunostaining for hCD31 (red) and isolectin B4 (green) using tissue samples at week 2. Scale bar: 50 μm. Differentiated human endothelial cells (ECs) identified as hCD31-positive cells (red) were observed in the $CD34^+$ (A, E) and NS (B) but not in the $CD34^-$ and PBS groups (C, D). Arrow, double-positive cells. E is higher magnification image of dotted box in A. (F) The number of human-derived ECs was significantly greater in the $CD34^+$ group compared with the other groups, as well as in the NS group greater than the $CD34^-$ or PBS group. $^{**}p<0.01$; $^{*}p<0.05$ ($n=6$ in each group). (G) The mRNA expressions of human vascular endothelial cadherin (hVE-cad) and hCD31 were detected from tissue RNA isolated from the perigraft site in the $CD34^+$ and NS groups. Posi, positive control from human umbilical vein endothelial cells (HUVECs); Nega, negative control with no RNA. (H–L) Representative immunostaining for HNA (red) and hOC (green) using samples collected at week 2. Scale bar: 50 μm. Differentiated human OBs identified as hOC-positive cells (green) were observed in the $CD34^+$ (H, L), NS (I), and $CD34^-$ group (J) but not in the PBS group (K). L is higher magnification image of dotted box in H. (M) The number of human-derived OB was significantly greater in the $CD34^+$ group compared with the other groups, as well as in the NS group greater than the $CD34^-$ or PBS group. $^{**}p<0.01$; $^{*}p<0.05$ ($n=6$ in each group). (N) The mRNA expression of hOsteocalcin (OC) and type I collagen (hCOL1) were detected from RNA isolated from tissues from the peribone tunnel site in the $CD34^+$ and NS groups. Posi, positive control from fetal bone; Nega, negative control with no RNA.

among any of the groups in BV/TV at weeks 0 and 2 (week 0: CD34+, 0.483±0.004; NS, 0.497±0.023; CD34−, 0.524±0.022; PBS, 0.514±0.027, respectively, p=NS; week 2: CD34+, 0.479±0.022; NS, 0.488±0.063; CD34−, 0.483±0.049; PBS, 0.500±0.059, respectively, p=NS), while the BV/TV at week 4 was significantly higher in the CD34+ group compared with the CD34− and PBS groups (week 4: CD34+, 0.651±0.038; NS, 0.589±0.049; CD34−, 0.476±0.069; PBS, 0.502±0.043, respectively, $p<0.05$ for CD34+ vs. CD34− or PBS group) (Fig. 5A). These results indicate that the ACL-derived CD34+ cells contribute to perigraft bone mass increase after ACL reconstruction.

Biomechanical Testing

Functional recovery of ACL reconstruction in each group was evaluated by failure load of biomechanical tensile test at week 8 postinjection. In all samples, the grafts were pulled out from the femoral or tibial bone tunnel subjected to failure load tests. Failure load of tensile test demonstrated that biomechanical strength was significantly higher in the CD34+ cell group compared with the other groups and the NS group was significantly higher compared with the CD34− and PBS groups; however, the uninjured control group showed a significantly greater result when compared with all the experimental groups (CD34+, 19.48±0.85; NS, 14.66±2.17; CD34−,

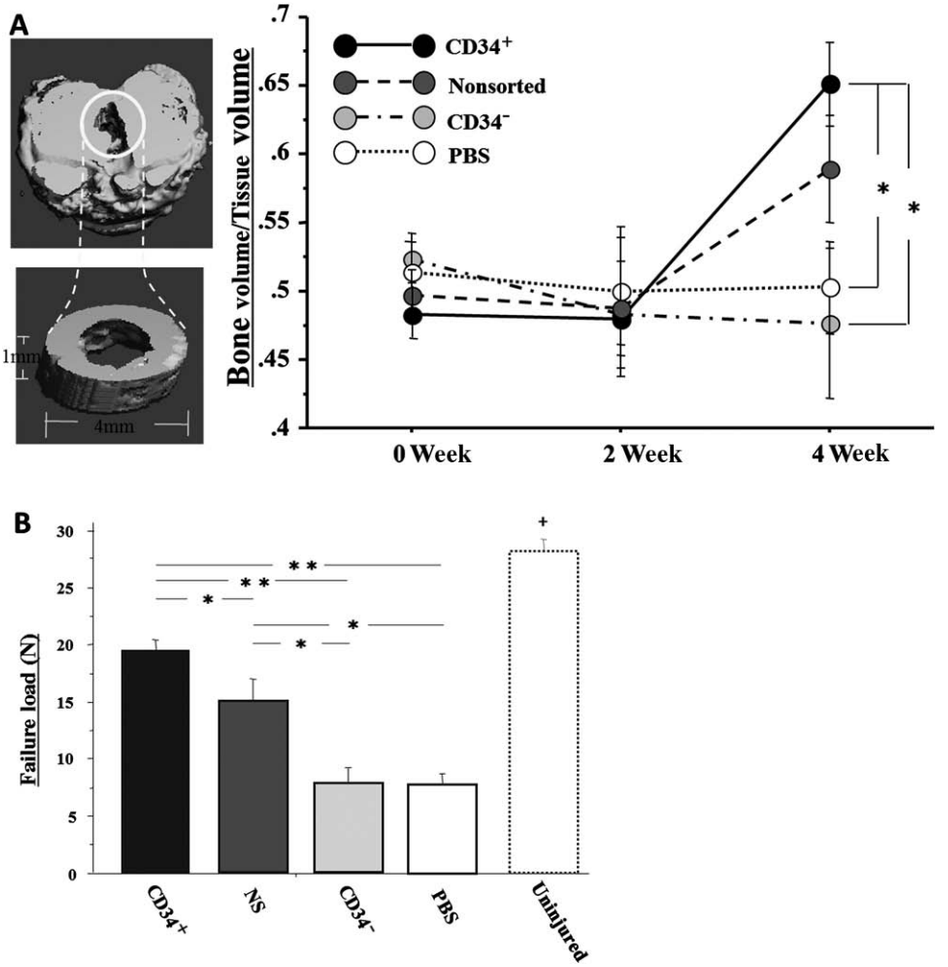

Figure 5. (A) The perigraft bone volume was evaluated with micro-CT. Transient perigraft bone mass decrease was observed in all groups at week 2. There was no significant difference among all groups in the bone volume/tissue volume (BV/TV) at weeks 0 and 2, while the BV/TV at week 4 was significantly higher in the CD34+ group compared with the CD34− or PBS group. *$p<0.05$ (n=6 in each group). (B) Biomechanical recovery of ligament injury in animals receiving ACL-derived cell transplantation. Failure load of tensile test demonstrated that biomechanical strength was significantly higher in the CD34+ cell group compared with the other groups and the NS group was significantly higher compared with the CD34− and PBS groups; however, the uninjured control group showed a significantly greater result when compared with all the experimental groups. **$p<0.01$; *$p<0.05$; +$p<0.01$ for all experimental groups (n=4 in each group).

7.64 ± 1.53; PBS, 7.67 ± 0.96; uninjured control, 27.54 ± 1.14, respectively, $p < 0.01$ for $CD34^+$ vs. $CD34^-$ or PBS group and uninjured verses all experimental groups, $p < 0.05$ for $CD34^+$ vs. NS group and NS vs. $CD34^-$ or PBS group) (Fig. 5B). These results indicate that the transplanted autologous graft in the immunodeficient rats were biomechanically healed with the administration of ACL-derived $CD34^+$ cells.

In Vitro Cell Proliferation Assay

To investigate the proliferation capabilities of each of the cell groups, we performed a cell proliferation assay with Cell Titer 96 Aqueous One Solution. The absorbance ratio of each of the cell groups to a control group was calculated to normalize the effect of the media. The cell proliferation assay showed that the $CD34^+$ group had a significantly greater proliferation ability than the other two groups. The NS cell group also demonstrated a significantly greater proliferation ability than the $CD34^-$ group ($CD34^+$, 2.13 ± 0.60; NS, 1.63 ± 0.84; $CD34^-$, 1.27 ± 0.49; no cell, 0.27 ± 0.04, respectively, $p < 0.01$ for $CD34^+$ vs. NS, $CD34^-$ or PBS group and NS vs. $CD34^-$ or PBS group) (Fig. 6A).

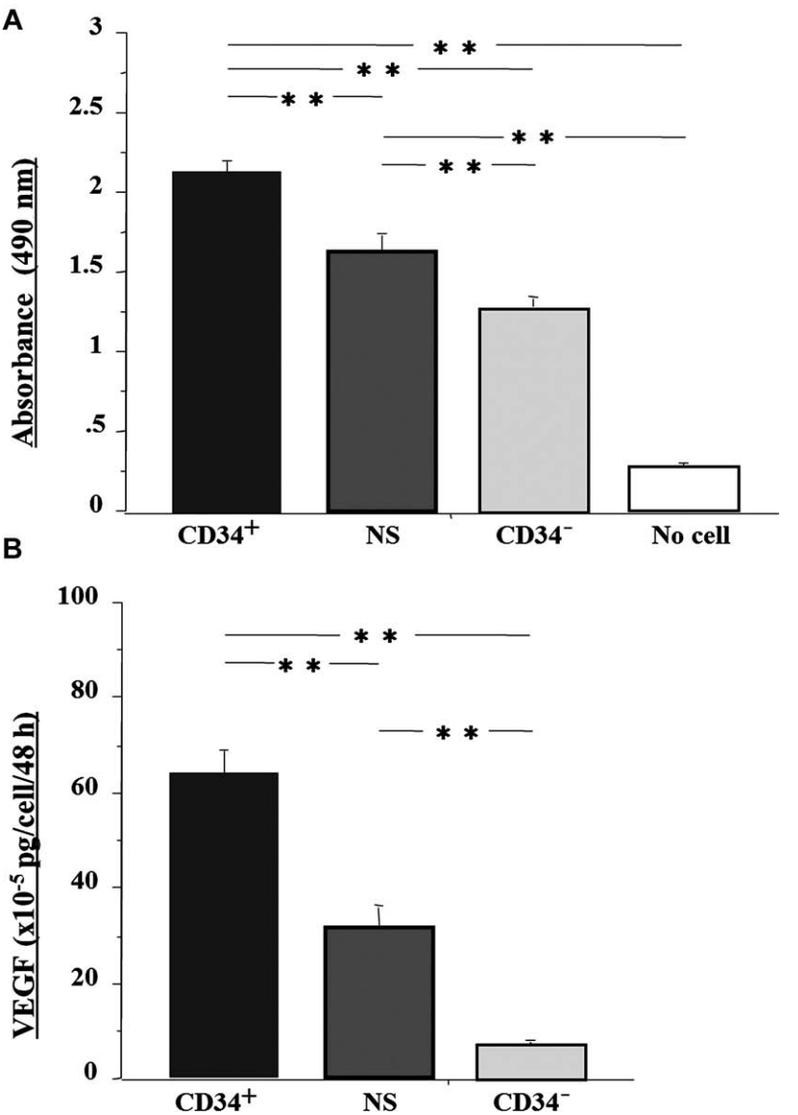

Figure 6. (A) The cell proliferation assay showed that the $CD34^+$ group had a significantly greater ability for proliferation than the other two groups. The NS was also significantly greater than the $CD34^-$ group. $^{**}p < 0.01$ ($n = 6$ in each group). (B) Enzyme-linked immunosorbent assay (ELISA) for vascular endothelial growth factor (VEGF) revealed that VEGF secretion in the $CD34^+$ group was significantly increased compared to the other two groups. The NS was also significantly greater than the $CD34^-$ group. $^{**}p < 0.01$ ($n = 6$ in each group).

VEGF Secretion Levels

VEGF levels were measured in the medium of the cell cultures using ELISA, which showed that VEGF levels in the $CD34^+$ group was significantly higher compared to the other two groups. The NS cell group was also significantly greater than the $CD34^-$ group ($CD34^+$, 63.5 ± 4.9; NS, 31.3 ± 3.4; $CD34^-$, 6.7 ± 0.5, respectively, $p < 0.01$ for $CD34^+$ vs. NS or $CD34^-$ group and NS vs. PBS group) (Fig. 6B).

DISCUSSION

This is the first report that we are aware that utilize ACL-derived cells to aid in the healing of ACL reconstruction. The study demonstrated that these certain populations of these ACL-derived cells can differentiate into ECs and OBs when injected into the joint capsules of reconstructed ACLs. The objective of this study was to develop a new strategy to accelerate the healing between graft tendon and bone after ACL reconstruction.

Initially, we examined the efficiency of incorporation into the perigraft site after the intracapuslar injection of each cell group. Our immunohistochemical evaluations showed that the greatest number of transplanted cells that migrated into the perigraft site were ACL-derived $CD34^+$ cells (Fig. 1). Stem cells, like bone marrow mesenchymal stem cells (BM-MSC) and synovial stem cells, have been reported to migrate to injured tissues after intracapuslar injection (1,13,17). This result could be explained by the fact that the $CD34^+$ cell marker is known as a hematopoietic stem/endothelial progenitor cell marker (2) and the ACL-derived cells isolated on the basis of CD34 showed that the $CD34^+$ cells demonstrated the best regenerative capacity among the other cell groups isolated ($CD34^-$ and unsorted cells) cells.

At week 2 after ACL reconstruction, the application of ACL-derived $CD34^+$ and NS cells had the potential to accelerate the early remodeling of tendon–bone healing histologically by forming a greater numbers of collagen fibers connecting the bone to the tendon and Col2-positive cells (chondrocytes) (Fig. 2). Tendon–bone healing has been reported to be enhanced with more perpendicular collagen fibers being deposited and the proliferation of cartilage-like tissue within the bone tunnels (29). Moreover, we investigated the therapeutic ability of the ACL-derived cells for their angiogenesis and osteogenesis potentials. The immunohistological results in this study indicated that the ACL-derived $CD34^+$ and NS cells could produce the intrinsic effect necessary to promote angiogenesis and osteogenesis (Fig. 3). These cells were also shown to be capable of differentiating into ECs and OBs at the perigraft sites (Fig. 4). In a previous study of ours, we have already shown that ACL-derived stem cells isolated from the site of ACL rupture have the potential for multilineage differentiation including osteogenic, chondrogenic, adipogenic, and endothelial differentiation in vitro (26), of which, osteogenic and endothelial differentiations are especially important for good quality bone-tendon healing (21). In fact, various cytokines and growth factors including VEGF (41), platelet-derived growth factor (PDGF) (22), fibroblast growth factor 2 (FGF2) (21), granulocyte colony-stimulating factor (G-CSF) (33), transforming growth factor-β (TGF-β) (40), bone morphogenetic protein 2 (BMP 2) (25), and BMP 7 (27) have recently received attention for their therapeutic potential to accelerate osteogenesis and/or angiogenesis for improving tendon–bone healing. Moreover, some stem/progenitor cells including BM-MSC (23,29,34) and synovial stem cells (15) have also received attention for their potential to accelerate osteogenesis and/or angiogenesis to help improve tendon–bone healing.

Furthermore, we evaluated perigraft bone volume using a micro-CT to reveal bone healing at the perigraft site. The perigraft bone mass was observed to decreased in all groups at week 2 (Fig. 5), which could be caused by graft fixation weakness or the activity immediately after surgery. That is, both ends of the grafted tendon were secured to the surrounding periosteum at the extra-articular tunnel exit sites at the distal femur and proximal tibia using 4-0 Ethibond sutures in this animal model (20), and after surgery the animals were allowed to move freely within the cage without fixating the reconstructed leg. At 4 weeks after ACL reconstruction, micro-CT evaluation showed that the ACL-derived $CD34^+$ cells contributed to an increase in bone mass at the perigraft sites. It has previously been reported that the healing quality of tendon–bone attachment is influenced by perigraft bone mass (11) and that tendon–bone attachment strength was directly related to perigraft bone mass after ACL reconstruction (38). Hence, our results obtained from the micro-CT appeared to highly correlate with our biomechanical results.

Finally, the functional healing between bone and graft after ACL reconstruction had been assessed by failure load of biomechanical tensile test at week 8 postreconstruction. Failure loads obtained in both the $CD34^+$ and NS groups were significantly higher compared with the $CD34^-$ and PBS groups (Fig. 5); however, in comparison with uninjured knees, only the $CD34^+$ group exhibited almost the same strength as the uninjured knees in failure load test. These results were supported by the histological findings which demonstrated better healing in the $CD34^+$ cell group when compared to the other groups. The ACL reconstructions in the immunodeficient rats were not only enhanced biologically with the administration of ACL-derived $CD34^+$ cells but also biomechanically. Previous studies have also reported that the maximum pullout load progressively increases as collagen fibers continue to grow and as the interface healing matures histologically (32).

In an attempt to clarify why the ACL-derived CD34+ cells had a superior influence on the healing of the ACL reconstructions, we performed in vitro assays to determine the cell's proliferation capacities and levels of VEGF secretion (Fig. 6). Both assays demonstrated, at least in part, potential mechanisms behind the beneficial effects imparted by the ACL-derived CD34+ cells. It has previously been reported that population doubling (PD) times exhibited by the ACL-derived CD34+ cells were significantly higher than the PD times exhibited by ACL-derived CD34− cells (26). In the current study, we revealed that the CD34+ cell group also had significantly greater capacities for cell proliferation when compared with the non-sorted and CD34− cells. The cell surface marker CD34 is considered a hematopoietic stem/endothelial progenitor cell marker (2), and CD34+ cells from the bone marrow and peripheral blood have been reported to secret greater amounts of VEGF than CD34− cells (24). We also confirmed that ACL-derived CD34+ cells could secret higher levels of VEGF than the non-sorted and CD34− cells in this study.

On the whole, the biological evaluations (Figs. 1–4) demonstrated that both the ACL-derived CD34+ and NS cells had the potential to promote tendon–bone healing, while the micro-CT and biomechanical evaluations (Fig. 5) demonstrated that the only the ACL-derived CD34+ cells had the ability to create a quality tendon–bone attachment. Furthermore, the in vitro studies indicated that the ACL-derived CD34+ cells showed increased cell proliferation capabilities and increased VEGF secretion levels (Fig. 6). We therefore came to the conclusion that only the ACL-derived CD34+ cells were highly effective for aiding the rapid recovery of ACL reconstructions.

The CD34+ cells isolated from bone marrow and peripheral blood have already been used in a clinical setting for the repair of various damaged tissues including lower limb ischemia, myocardial infarction, and nonunion fracture, because these cell populations have been recognized to be a rich population of hematopoietic/endothelial progenitor cells (2). As our previous study indicated, the ACL-derived CD34+ cells used in this study were considered to be derived from the vascularized area of the ACL (26), and therefore, the origin of the ACL-derived CD34+ cells may be the same as the bone marrow/peripheral blood-derived CD34+ cells.

Several limitations should be noted in this study. Firstly, although we have already clarified the multidifferentiation capacity of ACL-derived cells into ECs and OBs, we have not demonstrated whether the ACL-derived cells might have the potential to differentiate into fibroblasts to directly contribute to the graft tendon healing. Secondly, the rat model used in the present study is very small and the tendon–bone healing process occurs at a faster rate in rats than in humans. We need further studies to test the effectiveness of this application in a large-animal model to confirm its clinical feasibility. If the treatment of ACL-derived cells produces a clinical effect, it could improve rehabilitation and produce a better outcome for ligament reconstructions in general.

In conclusion, our results demonstrated that ACL-derived CD34+ cells isolated from the site of ACL rupture exhibited stem cell characteristics and may contribute to tendon–bone healing in ACL reconstruction. The present findings provide important clinical insight for regenerative medicine aimed at enhancing tendon–bone healing in ACL reconstruction, and the methods used in the current study could one day be translated into a clinically reasonable treatment regime to enhance ACL reconstruction repair.

ACKNOWLEDGMENTS: The authors are grateful for technical and scientific advice provided by James Cummins, Jessica Tebbets, and Michele Witt (SCRC). Funding for these studies were provided in part by the Henry J. Mankin endowed chair at the University of Pittsburgh and the William F. and Jean W. Donaldson Endowed Chair in Pediatric Orthopedic Surgery at Children's Hospital of Pittsburgh. The authors declare no conflict of interest.

REFERENCES

1. Agung, M.; Ochi, M.; Yanada, S.; Adachi, N.; Izuta, Y.; Yamasaki, T.; Toda, K. Mobilization of bone marrow-derived mesenchymal stem cells into the injured tissues after intraarticular injection and their contribution to tissue regeneration. Knee Surg. Sports Traumatol. Arthrosc. 14(12):1307–1314; 2006.
2. Asahara, T.; Murohara, T.; Sullivan, A.; Silver, M.; van der Zee, R.; Li, T.; Witzenbichler, B.; Schatteman, G.; Isner, J. M. Isolation of putative progenitor endothelial cells for angiogenesis. Science 275(5302):964–967; 1997.
3. Ballock, R. T.; Woo, S. L.; Lyon, R. M.; Hollis, J. M.; Akeson, W. H. Use of patellar tendon autograft for anterior cruciate ligament reconstruction in the rabbit: A long-term histologic and biomechanical study. J. Orthop. Res. 7(4):474–485; 1989.
4. Butler, D. L. Kappa Delta Award paper. Anterior cruciate ligament: Its normal response and replacement. J. Orthop. Res. 7(6):910–921; 1989.
5. Clancy Jr., W. G.; Narechania, R. G.; Rosenberg, T. D.; Gmeiner, J. G.; Wisnefske, D. D.; Lange, T. A. Anterior and posterior cruciate ligament reconstruction in rhesus monkeys. J. Bone Joint Surg. 63(8):1270–1284; 1981.
6. Cobellis, G.; Maione, C.; Botti, C.; Coppola, A.; Silvestroni, A.; Lillo, S.; Schiavone, V.; Molinari, A. M.; Sica, V. Beneficial effects of VEGF secreted from stromal cells in supporting endothelial cell functions: Therapeutic implications for critical limb ischemia. Cell Transplant. 19(11):1425–1437; 2010.
7. Crisan, M.; Deasy, B.; Gavina, M.; Zheng, B.; Huard, J.; Lazzari, L.; Peault, B. Purification and long-term culture of multipotent progenitor cells affiliated with the walls of human blood vessels: Myoendothelial cells and pericytes. Methods Cell Biol. 86:295–309; 2008.
8. Crisan, M.; Yap, S.; Casteilla, L.; Chen, C. W.; Corselli, M.; Park, T. S.; Andriolo, G.; Sun, B.; Zheng, B.; Zhang, L.; Norotte, C.; Teng, P. N.; Traas, J.; Schugar, R.; Deasy,

B. M.; Badylak, S.; Buhring, H. J.; Giacobino, J. P.; Lazzari, L.; Huard, J.; Peault, B. A perivascular origin for mesenchymal stem cells in multiple human organs. Cell Stem Cell 3(3):301–313; 2008.
9. Delay, B. S.; McGrath, B. E.; Mindell, E. R. Observations on a retrieved patellar tendon autograft used to reconstruct the anterior cruciate ligament. A case report. J. Bone Joint Surg. 84-A(8):1433–1438; 2002.
10. Grana, W. A.; Egle, D. M.; Mahnken, R.; Goodhart, C. W. An analysis of autograft fixation after anterior cruciate ligament reconstruction in a rabbit model. Am. J. Sports Med. 22(3):344–351; 1994.
11. Grassman, S. R.; McDonald, D. B.; Thornton, G. M.; Shrive, N. G.; Frank, C. B. Early healing processes of free tendon grafts within bone tunnels is bone-specific: A morphological study in a rabbit model. Knee 9(1):21–26; 2002.
12. Griffin, L. Y.; Agel, J.; Albohm, M. J.; Arendt, E. A.; Dick, R. W.; Garrett, W. E.; Garrick, J. G.; Hewett, T. E.; Huston, L.; Ireland, M. L.; Johnson, R. J.; Kibler, W. B.; Lephart, S.; Lewis, J. L.; Lindenfeld, T. N.; Mandelbaum, B. R.; Marchak, P.; Teitz, C. C.; Wojtys, E. M. Noncontact anterior cruciate ligament injuries: Risk factors and prevention strategies. J. Am. Acad. Orthop. Surg. 8(3):141–150; 2000.
13. Horie, M.; Sekiya, I.; Muneta, T.; Ichinose, S.; Matsumoto, K.; Saito, H.; Murakami, T.; Kobayashi, E. Intra-articular Injected synovial stem cells differentiate into meniscal cells directly and promote meniscal regeneration without mobilization to distant organs in rat massive meniscal defect. Stem Cells 27(4):878–887; 2009.
14. Howson, K. M.; Aplin, A. C.; Gelati, M.; Alessandri, G.; Parati, E. A.; Nicosia, R. F. The postnatal rat aorta contains pericyte progenitor cells that form spheroidal colonies in suspension culture. Am. J. Physiol. Cell Physiol. 289(6):C1396–1407; 2005.
15. Ju, Y. J.; Tohyama, H.; Kondo, E.; Yoshikawa, T.; Muneta, T.; Shinomiya, K.; Yasuda, K. Effects of local administration of vascular endothelial growth factor on properties of the in situ frozen–thawed anterior cruciate ligament in rabbits. Am. J. Sports Med. 34(1):84–91; 2006.
16. Kalka, C.; Masuda, H.; Takahashi, T.; Kalka-Moll, W. M.; Silver, M.; Kearney, M.; Li, T.; Isner, J. M.; Asahara, T. Transplantation of ex vivo expanded endothelial progenitor cells for therapeutic neovascularization. Proc. Natl. Acad. Sci. USA 97(7):3422–3427; 2000.
17. Kanaya, A.; Deie, M.; Adachi, N.; Nishimori, M.; Yanada, S.; Ochi, M. Intra-articular injection of mesenchymal stromal cells in partially torn anterior cruciate ligaments in a rat model. Arthroscopy 23(6):610–617; 2007.
18. Kawamoto, A.; Gwon, H. C.; Iwaguro, H.; Yamaguchi, J. I.; Uchida, S.; Masuda, H.; Silver, M.; Ma, H.; Kearney, M.; Isner, J. M.; Asahara, T. Therapeutic potential of ex vivo expanded endothelial progenitor cells for myocardial ischemia. Circulation 103(5):634–637; 2001.
19. Kawamoto, A.; Tkebuchava, T.; Yamaguchi, J.; Nishimura, H.; Yoon, Y. S.; Milliken, C.; Uchida, S.; Masuo, O.; Iwaguro, H.; Ma, H.; Hanley, A.; Silver, M.; Kearney, M.; Losordo, D. W.; Isner, J. M.; Asahara, T. Intramyocardial transplantation of autologous endothelial progenitor cells for therapeutic neovascularization of myocardial ischemia. Circulation 107(3):461–468; 2003.
20. Kawamura, S.; Ying, L.; Kim, H. J.; Dynybil, C.; Rodeo, S. A. Macrophages accumulate in the early phase of tendon–bone healing. J. Orthop. Res. 23(6):1425–1432; 2005.
21. Kohno, T.; Ishibashi, Y.; Tsuda, E.; Kusumi, T.; Tanaka, M.; Toh, S. Immunohistochemical demonstration of growth factors at the tendon–bone interface in anterior cruciate ligament reconstruction using a rabbit model. J. Orthop. Sci. 12(1):67–73; 2007.
22. Li, F.; Jia, H.; Yu, C. ACL reconstruction in a rabbit model using irradiated Achilles allograft seeded with mesenchymal stem cells or PDGF-B gene-transfected mesenchymal stem cells. Knee Surg. Sports Traumatol. Arthrosc. 15(10):1219–1227; 2007.
23. Lim, J. K.; Hui, J.; Li, L.; Thambyah, A.; Goh, J.; Lee, E. H. Enhancement of tendon graft osteointegration using mesenchymal stem cells in a rabbit model of anterior cruciate ligament reconstruction. Arthroscopy 20(9):899–910; 2004.
24. Majka, M.; Janowska-Wieczorek, A.; Ratajczak, J.; Ehrenman, K.; Pietrzkowski, Z.; Kowalska, M. A.; Gewirtz, A. M.; Emerson, S. G.; Ratajczak, M. Z. Numerous growth factors, cytokines, and chemokines are secreted by human CD34(+) cells, myeloblasts, erythroblasts, and megakaryoblasts and regulate normal hematopoiesis in an autocrine/paracrine manner. Blood 97(10):3075–3085; 2001.
25. Martinek, V.; Latterman, C.; Usas, A.; Abramowitch, S.; Woo, S. L.; Fu, F. H.; Huard, J. Enhancement of tendon–bone integration of anterior cruciate ligament grafts with bone morphogenetic protein-2 gene transfer: A histological and biomechanical study. J. Bone Joint Surg. 84-A(7):1123–1131; 2002.
26. Matsumoto, T., Ingham, M.S., Mifune, Y., Osawa, A., Logar, A., Usas, A., Kuroda, R., Kurosaka, M., Fu, F. H., and Huard, J. Isolation and characterization of human anterior cruciate ligament-derived vascular stem cells. Stem Cells Dev. 21(6):859–872; 2012.
27. Mihelic, R.; Pecina, M.; Jelic, M.; Zoricic, S.; Kusec, V.; Simic, P.; Bobinac, D.; Lah, B.; Legovic, D.; Vukicevic, S. Bone morphogenetic protein-7 (osteogenic protein-1) promotes tendon graft integration in anterior cruciate ligament reconstruction in sheep. Am. J. Sports Med. 32(7):1619–1625; 2004.
28. Nakamura, T.; Tsutsumi, V.; Torimura, T.; Naitou, M.; Iwamoto, H.; Masuda, H.; Hashimoto, O.; Koga, H.; Abe, M.; Ii, M.; Kawamoto, A.; Asahara, T.; Ueno, T.; Sata, M. Human peripheral blood CD34-positive cells enhance therapeutic regeneration of chronically injured liver in nude rats. J. Cell. Physiol. 227(4):1538–1552; 2012.
29. Ouyang, H. W.; Goh, J. C.; Lee, E. H. Use of bone marrow stromal cells for tendon graft-to-bone healing: Histological and immunohistochemical studies in a rabbit model. Am. J. Sports Med. 32(2):321–327; 2004.
30. Payne, T. R.; Oshima, H.; Okada, M.; Momoi, N.; Tobita, K.; Keller, B. B.; Peng, H.; Huard, J. A relationship between vascular endothelial growth factor, angiogenesis, and cardiac repair after muscle stem cell transplantation into ischemic hearts. J. Am. Coll. Cardiol. 50(17):1677–1684; 2007.
31. Petersen, W.; Petersen, F.; Tillmann, B. Structure and vascularization of the acetabular labrum with regard to the pathogenesis and healing of labral lesions. Arch. Orthop. Trauma Surg. 123(6):283–288; 2003.
32. Rodeo, S. A.; Suzuki, K.; Deng, X. H.; Wozney, J.; Warren, R. F. Use of recombinant human bone morphogenetic protein-2 to enhance tendon healing in a bone tunnel. Am. J. Sports Med. 27(4):476–488; 1999.
33. Sasaki, K.; Kuroda, R.; Ishida, K.; Kubo, S.; Matsumoto, T.; Mifune, Y.; Kinoshita, K.; Tei, K.; Akisue, T.; Tabata, Y.;

Kurosaka, M. Enhancement of tendon–bone osteointegration of anterior cruciate ligament graft using granulocyte colony-stimulating factor. Am. J. Sports Med. 36(8):1519–1527; 2008.
34. Soon, M. Y.; Hassan, A.; Hui, J. H.; Goh, J. C.; Lee, E. H. An analysis of soft tissue allograft anterior cruciate ligament reconstruction in a rabbit model: A short-term study of the use of mesenchymal stem cells to enhance tendon osteointegration. Am. J. Sports Med. 35(6):962–971; 2007.
35. Tavian, M.; Zheng, B.; Oberlin, E.; Crisan, M.; Sun, B.; Huard, J.; Peault, B. The vascular wall as a source of stem cells. Ann. N. Y. Acad. Sci. 1044:41–50; 2005.
36. Tohyama, H.; Yoshikawa, T.; Ju, Y. J.; Yasuda, K. Revascularization in the tendon graft following anterior cruciate ligament reconstruction of the knee: Its mechanisms and regulation. Chang Gung Med. J. 32(2):133–139; 2009.
37. Weiss, J. A.; Woo, S. L.; Ohland, K. J.; Horibe, S.; Newton, P. O. Evaluation of a new injury model to study medial collateral ligament healing: Primary repair versus nonoperative treatment. J. Orthop. Res. 9(4):516–528; 1991.
38. Wen, C. Y.; Qin, L.; Lee, K. M.; Chan, K. M. Perigraft bone mass and connectivity as predictors for the strength of tendon-to-bone attachment after anterior cruciate ligament reconstruction. Bone 45(3):545–552; 2009.
39. Woo, S. L.; Inoue, M.; McGurk-Burleson, E.; Gomez, M. A. Treatment of the medial collateral ligament injury: II. Structure and function of canine knees in response to differing treatment regimens. Am. J. Sports Med. 15(1):22–29; 1987.
40. Yasuda, K.; Tomita, F.; Yamazaki, S.; Minami, A.; Tohyama, H. The effect of growth factors on biomechanical properties of the bone-patellar tendon–bone graft after anterior cruciate ligament reconstruction: A canine model study. Am. J. Sports Med. 32(4):870–880; 2004.
41. Yoshikawa, T.; Tohyama, H.; Katsura, T.; Kondo, E.; Kotani, Y.; Matsumoto, H.; Toyama, Y.; Yasuda, K. Effects of local administration of vascular endothelial growth factor on mechanical characteristics of the semitendinosus tendon graft after anterior cruciate ligament reconstruction in sheep. Am. J. Sports Med. 34(12):1918–1925; 2006.
42. Zheng, B.; Cao, B.; Crisan, M.; Sun, B.; Li, G.; Logar, A.; Yap, S.; Pollett, J. B.; Drowley, L.; Cassino, T.; Gharaibeh, B.; Deasy, B. M.; Huard, J.; Péault, B. Prospective identification of myogenic endothelial cells in human skeletal muscle. Nat. Biotechnol. 25(9):1025–1034; 2007.